Journal of Alloys and Compounds 596 (2014) 69–72

Contents lists available at ScienceDirect

Journal of Alloys and Compounds

journal homepage: www.elsevier.com/locate/jalcom

Tunable magnetic transition and reversible magnetocaloric effects at room temperature in transition-metal-oxyfluorides $CrO_{2-x}F_x$

Weijun Ren [a,*], Bing Li [a], Wen Liang [b], Changqing Jin [b], Zhidong Zhang [a]

[a] Shenyang National Laboratory for Materials Science, Institute of Metal Research, Chinese Academy of Sciences, Shenyang 110016, China
[b] Beijing National Laboratory for Condensed Matter Physics, and Institute of Physics, Chinese Academy of Sciences, Beijing 100190, China

ARTICLE INFO

Article history:
Received 14 January 2014
Received in revised form 24 January 2014
Accepted 27 January 2014
Available online 2 February 2014

Keywords:
CrO_2
Magnetocaloric effect
Relative cooling power
High-pressure synthesis

ABSTRACT

We report the tuning of magnetic transition and associated reversible magnetocaloric effect in $CrO_{2-x}F_x$ by manipulating the doping levels. At $x = 0.12$, the magnetic transition occurs at room temperature, with magnetic-entropy changes of around 4 J kg^{-1} K^{-1} and relative cooling power of 388 J kg^{-1} at magnetic-field changes from 0 to 50 kOe. The reversibility is verified by negligible thermal and magnetic hysteresis, as well as the positive slope at Arrott plots. The complete phase diagram for electronic and magnetic states is drawn for $CrO_{2-x}F_x$. This work indicates $CrO_{1.88}F_{0.12}$ is a promising candidate for room temperature magnetic refrigeration because of the nature of second-order transition and abundance of elements involved.

1. Introduction

As the environmental and energy concerns grow, magnetic refrigeration attracts much attention because of its environmentally friendly and energy-efficient features [1–3]. The magnetic refrigeration is regarded as a promising alternative to currently used vapor-cycle refrigeration. Since Brown et al. showed that rare earth Gd displays an appealing magnetic refrigeration performance, intensive efforts have been devoting to designing and searching better magnetic refrigeration materials [4,5]. In 1997, Pecharsky and Gschneidner discovered giant magnetocaloric effect (MCE) in $Gd_5Si_2Ge_2$ via a route of magneto-structural coupled first-order magnetic transition [6]. Successively, giant MCEs have been reported in many systems, such as $La(Fe_{1-x}Si_x)_{13}$ [7], $MnFe(P_{1-x}As_x)$ [8], MnAs-based compounds [9], and colossal magnetoresistance manganites [10,11]. More recently, MnCoGe related compounds were reported to undergo a magneto-structural coupled transition from the paramagnetic (PM) Ni_2In-type phase to the ferromagnetic (FM) TiNiSi-type phase, accompanying giant MCEs [12,13]. However, their inherent magnetic and thermal hystereses are obstacles to magnetic refrigeration application and most of magnetic refrigerators reported are based on Gd [14]. Therefore, Gd has been regarded as the prototype and the best materials for magnetic refrigeration so far.

The larger MCEs based on second-order phase transitions are an alternative approach to energy-efficient magnetic refrigeration, paralleling with the first-order counterpart where a compromise has been done between giant MCEs and considerable hysteresis effects [15]. Thus, it is advisable to explore advanced MCE materials with second-order transitions. Moreover, the global shortage of rare earth elements has been aggravated by the rapidly increasing demand on rare earth permanent magnets [16]. Consequently, the rare-earth-free MCE materials are highly desirable from the viewpoint of practical application. We have found Mn_5PB_2 is a promising system where larger reversible MCE might be obtained by further optimizing the composition [17]. A large MCE was also found in another transition-metal-boride $AlFe_2B_2$ system [18]. CrO_2, one of the simplest binary oxides, is a correlated FM half-metal [19], with magnetization of around 2 μ_B, explained by dynamic double-exchange interaction in terms of LDA + U electronic structure calculation [20]. It undergoes a second-order PM to FM transition at Curie temperature T_C of around 390 K [21]. It has been applied as a kind of magnetic recording medium for magnetic tapes and is also believed as a promising spintronic material [22,23]. A pretty large MCE has been found at its T_C (~390 K) at quite low magnetic-field change of 15 kOe [24]. It is interesting to look at whether the magnetic transition can be suppressed down to room temperature for application proposal and how large MCE can be obtained. In this work, we report there is the reduced T_C and reversible MCE in $CrO_{2-x}F_x$ ($x = 0.10, 0.12, 0.14$).

* Corresponding author.
E-mail address: wjren@imr.ac.cn (W. Ren).

http://dx.doi.org/10.1016/j.jallcom.2014.01.198
0925-8388/

2. Experimental procedure

The $CrO_{2-x}F_x$ ($x = 0.10, 0.12, 0.14$) compounds were prepared at high-pressure and high-temperature conditions [21,25]. The synthesis and structural characterizations were described elsewhere in details [26]. The magnetization was measured at MPMS-XL, Quantum Design, with temperature varying at rate of 5 K/min, in the settle mode. The isothermal magnetization and demagnetization were measured in the hysteresis mode at constant temperature. The magnetic-entropy change was calculated in terms of Maxwell relation [1]

$$\Delta S(T_{av}, H) = \int_0^H \left(\frac{\partial M}{\partial T}\right)_H dH \approx \frac{1}{\Delta T}\int_0^H [M(T_{i+1}, H) - M(T_i, H)]dH \quad (1)$$

Here $T_{av} = (T_{i+1} + T_i)/2$ denotes the average temperature of T_{i+1} and T_i. ΔT is the temperature difference between two isotherms involved.

3. Results and discussion

In Fig. 1, the temperature (T) dependencies of derivative of magnetization M, dM/dT, are displayed for $CrO_{2-x}F_x$ ($x = 0.10, 0.12, 0.14$) at field-cooled (FC) and field-warmed (FW) conditions, respectively. The negative peaks in dM/dT–T are defined as T_C for each samples and it can be seen that T_C is 315, 290, and 200 K, for $x = 0.10$, 0.12, 0.14, respectively. The heavier F doping greatly drives the magnetic transition down to lower temperatures, which is resulted from that the partial Cr^{4+}–Cr^{4+} ferromagnetic interactions were substituted by antiferromagnetic (AFM) Cr^{4+}–Cr^{3+} interactions because of F^- doping. The existence of the AFM interaction was proved by the AFM long range ordering and the related magnetic phase transition in $CrO_{2-x}F_x$ with $x \geqslant 0.14$ [21,26]. Usually, the expansion of lattice causes the decrease of interaction strength and the consequent T_C. However, both experimental and theoretical studies indicated T_C of CrO_2 decreased with the contrary lattice contraction when pressure was applied [27,28]. Thus, the lattice expansion of $CrO_{2-x}F_x$ seems not to be one of the critical factors for decreasing T_C. In our experimental resolution, there is no obvious thermal hysteresis observed at the magnetic transitions for these three samples. This also suggests the magnetic transition is of second-order.

A series of magnetic isotherms were measured around T_C on each sample, as shown in Fig. 2(a) for $x = 0.10$, (c) for $x = 0.12$, and (d) for $x = 0.14$, respectively. The magnetization rapidly increases at low fields and shows a tendency to saturate with increasing fields. However, they are not saturated even at magnetic fields up to 50 kOe. This might be ascribed to the microstructure and magnetic anisotropy. It is well-known that the magnetization of CrO_2 is extremely dependent on its microstructure [24,25]. Only in the optimized synthesis conditions, the magnetization could be close to the theoretical magnitude of 2 μ_B. The starting material CrO_2 we used is pretty magnetically soft and the magnetization is nearly 2 μ_B at 5 K. It is needle-like with aspect ratio around 10:1, whereas $CrO_{2-x}F_x$ exhibit almost isotropic microstructure, according to our transmission electronic microscopy study previously reported in Ref. [26]. Fig. 2(b) displays M–H isotherm at 322 K measured on increasing and decreasing field for $x = 0.10$, with temperature is close to its T_C. It can be seen that the magnetization and demagnetization isotherms nearly coincide, i.e., there is no magnetic hysteresis around the transition temperature. Shown in Fig. 3 are the magnetic-entropy changes, $-\Delta S$ calculated by using Eq. (1) for $x = 0.10$, $x = 0.12$, and $x = 0.14$ at the magnetic-field changes from 0 to 50 kOe. The maximum of $-S$ occurs around T_C, 3.9 J kg^{-1} K^{-1} at 320 K for $x = 0.10$, 3.8 J kg^{-1} K^{-1} at 300 K for $x = 0.12$, and 2.8 J kg^{-1} K^{-1} at 226 K for $x = 0.14$, respectively. These values are inferior to the maximum $-\Delta S_m$ of 7.7 J kg^{-1} K^{-1} at 307 K for $AlFe_2B_2$ among the transition based materials with the second order magnetic phase transitions [18], and that of 4.9 J kg^{-1} K^{-1} at 300 K for Mn_5PB_2 [17]. However, the full-width at half-maximum (*fwhm*) of the $-\Delta S$ peak for $CrO_{2-x}F_x$ is very large, for example, it is about 102 K for $CrO_{1.88}F_{0.12}$. In other word, the temperature span for $-\Delta S$ larger than 1.9 J kg^{-1} K^{-1} is 102 K. From Fig. 5 in Ref. [18], that is about 55 K for $AlFe_2B_2$ when $-\Delta S$ is larger than the same value. Thus, a large relative cooling power (RCP), as the product of $-\Delta S_m$ and *fwhm*, 388 J kg^{-1} was obtained for $CrO_{1.88}F_{0.12}$. It is much larger than that of 210 J kg^{-1} for $AlFe_2B_2$ [18] and 230 J kg^{-1} for Mn_5PB_2 [17]. Compared with pure CrO_2, $-\Delta S_m$ of 5.1 J kg^{-1} K^{-1} at 390 K under magnetic-field changes of 15 kOe, the magnetic-entropy changes for $CrO_{2-x}F_x$ with F doping are relatively smaller [24]. It was reported that the magnetic-entropy changes are very sensitive to the microstructure for CrO_2 [24]. The needle-like sample has two times larger magnetic-entropy changes than ball-milled one that may be less anisotropic. This is supported by the X-ray magnetic circular dichroism observation on the film form [29]. Thus, it seems that the smaller magnitudes of magnetic-entropy changes in the present samples are associated with their isotropic microstructure. In fact, the microstructure dependence of magnetic-entropy changes exists also in intermetallic Tb_3Co we reported before [30]. Recently, we have proposed an alternative evaluation method for magnetic-entropy change, expressed as [31]

$$\Delta S = -\frac{\alpha_0}{2}[M(T,H)^2 - M_s(T)^2] \quad (2)$$

where α_0 is the inverse of Curie–Weiss constant and M_s is spontaneous magnetization. It allows us to predict the magnitude of $-\Delta S$ after the microstructural optimization. In a magnetic material, α_0 characterizes the feature of transition that is usually subjected to extrinsic factors such as microstructure and crystalline imperfection, whereas M is more intrinsic. α_0 was determined to be 100 Oe (emu/g)$^{-1}$ K^{-1} and M (398 K, 15 kOe) is around 30 emu/g for CrO_2. Thus, the magnetic-entropy change was evaluated as 4.5 J kg^{-1} K^{-1}, by using the above equation, which is well consistent with the results obtained from Maxwell relation. Then, by assuming the same transition features, i.e., α_0 for $x = 0.10$, the magnetic-entropy change is evaluated as 8 J kg^{-1} K^{-1} with M of about 40 emu/g at 15 kOe (Fig. 2(b)), which is 4 times larger than the currently observed value.

Within the Landau phase transition theory, the Gibbs free energy of a magnetic material in an applied magnetic field can be written as [31]

$$G = G_0 + \frac{1}{2}\alpha_0(T - T_0)M^2 + \frac{1}{4}\beta M^4 - MH \quad (3)$$

where H, M and G_0 are the magnetic field, the magnetization and the free energy in the paramagnetic state in the absence of a magnetic field, respectively; T_0 is the Curie–Weiss temperature; α_0 and β are the second order and fourth-order order-parameter coefficients, respectively. Sign of β is an indication of the nature of a magnetic transition. $\beta > 0$ is for a second-order transition whereas $\beta < 0$

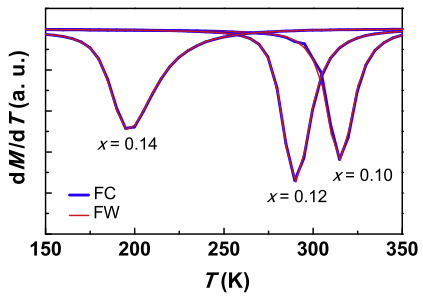

Fig. 1. Temperature dependencies of derivative of magnetization are displayed for $CrO_{2-x}F_x$ ($x = 0.10, 0.12, 0.14$) at FC-FW conditions.

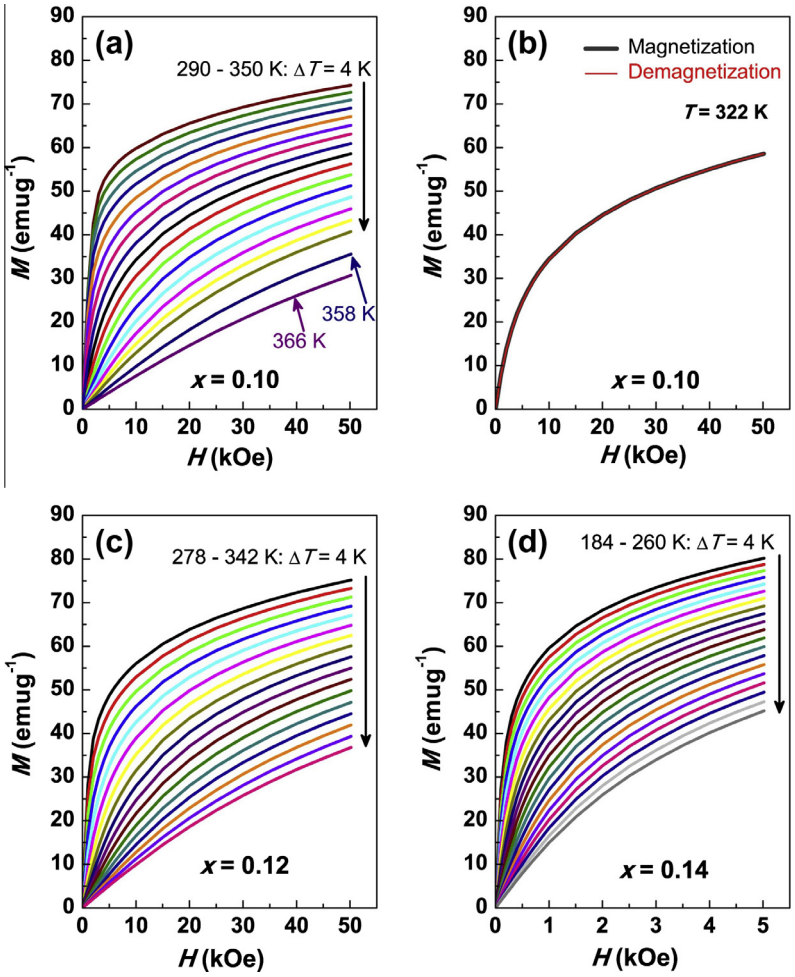

Fig. 2. Isothermal magnetization curves around T_C: (a) for $x = 0.10$, (c) for $x = 0.12$, and (d) for $x = 0.14$, respectively. (b) The highlight of the magnetization isotherm and demagnetization isotherm at 322 K for $x = 0.10$.

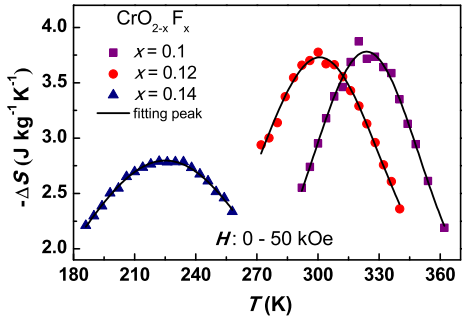

Fig. 3. Magnetic-entropy changes for $x = 0.10$, $x = 0.12$, and $x = 0.14$ at the magnetic-field changes from 0 to 50 kOe.

for a first-order transition. $\beta = 0$ occurs at critical point. By performing $(\frac{\partial G}{\partial M})_{H,T} = 0$, the equation of state is obtained as

$$\alpha_0(T - T_0)M + \beta M^3 = H \quad (4)$$

Obviously, the slope (β) in plot of M^2 versus H/M directly characterizes the nature of a magnetic phase transition. Such method is called Arrott plots and has been broadly used as a criterion to verify the reversibility of a MCE material. Based on the magnetization isotherms shown above, the Arrott plots [32], M^2 with H/M, are displayed in Fig. 4 (a) for $x = 0.10$, (b) for $x = 0.12$, and (c) for $x = 0.14$, respectively. They all display the positive slope at Arrott plots, i.e. $\beta > 0$, which is suggestive of the nature of second-order transitions. This is consistent with the temperature dependencies of FC-FW magnetization shown in Fig. 1. In Fig. 5, we draw the phase diagram for electronic and magnetic states of $CrO_{2-x}F_x$, also according to the data obtained in the previous reports [21,26]. With increasing F-doping content, T_C is reduced nearly linearly. At about $x = 0.14$, the AFM ordering develops at lower temperature. T_t where AFM insulator undergoes a transition to FM half-metal is not elevated too much when x is increased from 0.14 to 0.20. At x of 0.10, 0.12 and 0.14, there is a F^- stripe-phase with superlattice modulation of (1/3, 0, 1/3) and (−1/3, 0, 1/3), which is stable even at 573 K. The tunability of T_C in $CrO_{2-x}F_x$ by the F contents allows us to design MCE materials in quite broad temperature spans ranging from 200 to 400 K. The magnetic-entropy change associated with AFM to FM transition has been evaluated before [33].

To summarize, magnetic phase transitions and the MCE of $CrO_{2-x}F_x$ ($x = 0.10$, 0.12, 0.14) have been studied. The magnetic transition is tuned by F content and it takes place at room temperature when $x = 0.12$. Reversible MCEs are obtained around T_C, with the maximum $-\Delta S$ of around 4 J kg^{-1} K^{-1} and RCP of 388 J kg^{-1} at magnetic-field changes from 0 to 50 kOe. The complete phase diagram has been drawn, where AFM ordering emerges at $x = 0.14$ at lower temperatures. The MCEs might be improved by optimizing the microstructures. This system is promising as a candidate of

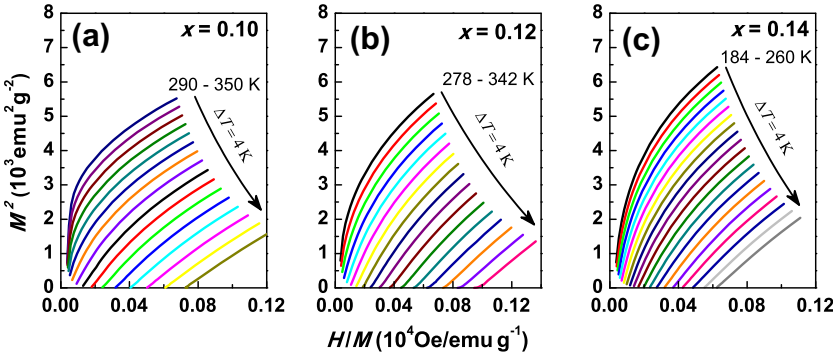

Fig. 4. Arrott plots around T_C with step of 4 K: (a) for $x = 0.10$ from 290 to 350 K, (b) for $x = 0.12$ from 278 to 342 K, and (c) for $x = 0.14$ from 184 to 260 K.

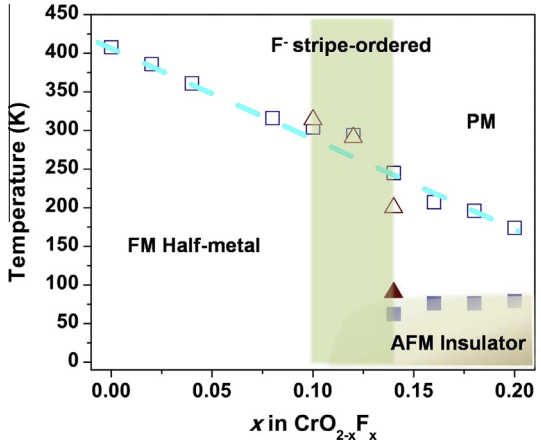

Fig. 5. Phase diagram of $CrO_{2-x}F_x$. The data points shown in squares are from Ref. [21] while those in triangles from the present work. The vertical shadow shows the region with F^- stripes order.

energy-efficient magnetic refrigerant at room temperature due to the reversibility and abundant availability of forming elements.

Acknowledgments

This work has been supported by the National Basic Research Program No. 2012CB619404, the Ministry of Science and Technology of China and the National Natural Science Foundation of China under Grant No. 51331006.

References

[1] A.M. Tishin, Y.I. Spichkin, The Magnetocaloric Effect and its Applications, IOP Publishing Ltd., Bristol, 2003.
[2] K.A. Gschneidner Jr., V.K. Pecharsky, A.O. Tsokol, Rep. Prog. Phys. 68 (2005) 1479.
[3] V. Franco, J.S. Blazquez, B. Ingale, A. Conde, Annu. Rev. Mater. Res. 42 (2012) 305.
[4] G.V. Brown, J. Appl. Phys. 47 (1976) 3673.
[5] S.Y. Dankov, A.M. Tishin, V.K. Pecharsky, K.A. Gschneidner Jr., Phys. Rev. B 57 (1998) 3478.
[6] V.K. Pecharsky, K.A. Gschneidner Jr., Phys. Rev. Lett. 78 (1997) 4494.
[7] F.X. Hu, B.G. Shen, J.R. Sun, Z.H. Cheng, G.H. Rao, X.X. Zhang, Appl. Phys. Lett. 78 (2001) 3675.
[8] O. Tegus, E. Brück, K.H.J. Buschow, F.R. de Boer, Nature 415 (2002) 150.
[9] H. Wada, Y. Tanabe, Appl. Phys. Lett. 79 (2001) 3302.
[10] M.H. Phan, S.C. Yu, J. Magn. Magn. Mater. 308 (2007) 325.
[11] A.N. Ulyanov, J.S. Kim, Y.M. Kang, D.G. Yoo, S.I. Yoo, J. Appl. Phys. 104 (2008) 113916.
[12] N.T. Trung, V. Biharie, L. Zhang, L. Caron, K.H.J. Buschow, E. Brück, Appl. Phys. Lett. 96 (2010) 162507.
[13] E.K. Liu, W.H. Wang, L. Feng, W. Zhu, G.J. Li, J.L. Chen, H.W. Zhang, G.H. Wu, C.B. Jiang, H.B. Xu, F.R. de Boer, Nat. Commun. 3 (2012) 873.
[14] K.A. Gschneidner Jr., V.K. Pecharsky, Int. J. Refrig. 31 (2008) 945.
[15] N.H. Dung, Z.Q. Ou, L. Caron, L. Zhang, D.T. CamThan, G.A. de Wijs, R.A. de Groot, K.H.J. Buschow, E. Brück, Adv. Energy Mater. 1 (2011) 1215.
[16] O. Gutfleisch, M.A. Willard, E. Brück, C.H. Chen, S.G. Sankar, J.P. Liu, Adv. Mater. 23 (2011) 821.
[17] Z.G. Xie, D.Y. Geng, Z.D. Zhang, Appl. Phys. Lett. 97 (2010) 202504.
[18] X.Y. Tan, P. Chai, C.M. Thompson, M. Shatruk, J. Am. Chem. Soc. 135 (2013) 9553.
[19] T. Tsujioka, T. Mizokawa, J. Okamoto, A. Fujimori, M. Nohara, H. Takagi, K. Yamaura, M. Takano, Phys. Rev. B 56 (1997) R15509.
[20] M.A. Korotin, V.I. Anisimov, D.I. Khomskii, G.A. Sawatzky, Phys. Rev. Lett. 80 (1998) 4305.
[21] B.L. Chamberland, Crit. Rev. Solid State Mater. Sci. 7 (1977) 1.
[22] J.M.D. Coey, M. Venkatesan, J. Appl. Phys. 91 (2002) 8345.
[23] R.S. Keizer, S.T.B. Goennenwein, T.M. Klapwijk, G. Miao, G. Xiao, A. Gupta, Nature (London) 439 (2006) 825.
[24] X.Y. Zhang, Y.J. Chen, L.Y. Lv, Z.Y. Li, J. Phys.: Condens. Matter 18 (2006) L559.
[25] A. Bajpaia, A.K. Nigam, Appl. Phys. Lett. 87 (2005) 222502.
[26] B. Li, Y.N. Chen, H. Wang, W. Liang, G.Y. Liu, W.J. Ren, C.F. Li, Z.Q. Liu, G.H. Rao, C.Q. Jin, Z.D. Zhang, Chem. Commun. 50 (2014) 799.
[27] V.A. Sidorov, A.V. Rakhmanina, O.A. Morya, Solid State Comm. 139 (2006) 360.
[28] S.F. Matar, G. Demazeau, Chem. Phys. Lett. 407 (2005) 516.
[29] E. Goering, A. Bayer, S. Gold, G. Schültz, M. Rabe, U. Rüdiger, G. Güntherodt, Phys. Rev. Lett. 88 (2002) 207203.
[30] B. Li, J. Du, W.J. Ren, W.J. Hu, Q. Zhang, D. Li, Z.D. Zhang, Appl. Phys. Lett. 92 (2008) 242504.
[31] B. Li, H. Meng, W. Ren, Z. Zhang, Europhys. Lett. 97 (2012) 57002.
[32] A. Arrott, Phys. Rev. 108 (1957) 1394.
[33] B. Li, W. Liang, W.J. Ren, W.J. Hu, J. Li, C.Q. Jin, Z.D. Zhang, Appl. Phys. Lett. 100 (2012) 242408.